University of Calgary

Department of Physics and Astronomy

# Advancing the Control for a Highly Maneuverable Autonomous Underwater Vehicle (HM-AUV)

By

Mobina Jamali

An undergraduate thesis submitted in partial fulfillment of the requirements for the degree of Bachelor of Science (B.Sc) in Physics and Astronomy

Supervisor

Dr. Alex Ramirez-Serrano

April 2023

**Abstract**

Autonomous Underwater Vehicles (AUVs) have become increasingly important in various ocean-related applications, and the ability to control the motion of AUVs with high accuracy and reliability is crucial for the success of these applications. This paper presents a comprehensive study of the dynamic modeling, control, and simulation of a Highly Maneuverable Autonomous Underwater Vehicle (HM-AUV) using the Newton-Euler formalism and PID control laws. The specific three thruster configuration with variable thrust vectoring of the HM-AUV is supposed to enable it to control all six degrees of freedom (6 DOF) and give the vehicle high maneuverability to perform acrobatic motions. While the dynamic model of the HM-AUV considers the hydrodynamic properties and inertial effects to provide an accurate representation of its environment and motion, the PID controller is designed based on the dynamic model and takes into account the thrusters' dynamics, providing independent and time variable orientation for each thruster. The simulation results for logarithmic spiral trajectory demonstrate the effectiveness of the proposed dynamic model and the PID controller in controlling the AUV's motion, achieving complex trajectories.

Overall, this work provides valuable insights into the design and implementation of control strategies for AUVs which can be applied to various applications, contributing to the advancement of ocean-related technologies, and addressing various challenges in underwater exploration, environmental monitoring, and other fields.

Keywords: Autonomous Underwater Vehicles, Dynamic Model, Thrust Vectoring, Control, PID, HM-AUV

**Acknowledgements**

I would like to express my sincere gratitude to several individuals who have played an important role in the completion of this project. First, I would like to thank my supervisor Dr. Alex, whose guidance and support have been invaluable throughout this research endeavor. Thank you for introducing the magical world of Robotics to me and let me find my passion and follow it! I would also like to extend my gratitude to my family members, friends and my love who have provided me with their unwavering encouragement, and emotional support during the ups and downs of this project. Furthermore, I would like to acknowledge Mr. Ali Kadkhodaei and Dr. Reza Hasan Zadeh, the authors of the paper "Inspection of Undersea Oil and Gas Pipelines by New Variable Thrust Vector Underwater Robotic Platform", whose insights and findings have provided the foundation for much of the analysis in this work and their technical support and advice from thousands of miles away, helped me a lot in the implementation of this project.

**Table of Contents**

## Introduction

Autonomous Underwater Vehicle (AUV) is a type of robot that is designed to operate underwater without the need for human intervention. An AUV typically consists of a body, propulsion system, sensors, and a computer system. The propulsion system is usually an electric motor that drives a propeller or a set of thrusters. The sensors on an AUV are used to collect data about the surrounding environment, and the computer system is responsible for controlling the vehicle's movement and processing the sensor data. AUVs are pre-programmed with a set of instructions that determine their mission objectives, and the computer system uses the sensor data to navigate the AUV to its destination while avoiding obstacles and adjusting its trajectory based on the environment. AUVs are typically launched from a surface vessel or from shore and can operate at depths of up to 6,000 meters [1,2].

AUVs are increasingly popular for marine applications, as they can operate in harsh environments where traditional manned vehicles cannot. This allows them to perform tasks such as oceanographic surveys, underwater inspections, and exploration. Due to communication difficulties underwater, full autonomy is essential for these vehicles to plan their own trajectory based on mission and environmental conditions. However, control and autonomy for AUVs remain an area of active research, and despite advancements in technology, their maximum potential has not been reached. Diverse techniques have been used over the years for the control of underwater vehicles. Regulating the movement of Autonomous Underwater Vehicles (AUVs) poses one of the most significant challenges in AUV technology. Unlike surface vehicles, AUVs must take all six degrees of freedom into account, which includes position (x, y, and z) and attitude (roll, pitch, and yaw), as they navigate through three-dimensional underwater environments. The movement of AUVs through water, a viscous fluid, requires the consideration of drag. Moreover, the water surrounding the vehicle accelerates when it moves, causing additional forces and moments known as added mass to come into play. Due to the complexity of the underwater environment and the limitations of communication with the vehicle, trajectory planning and controlling these vehicles in underwater environments is a difficult endeavor [3,4]. Developing an effective control system that can guide

the AUV through these environments is a difficult task that requires a complex dynamic algorithm. Designing such an algorithm involves many factors, including the modeling of the vehicle's dynamics, accounting for external disturbances, and optimizing the AUV's path to achieve specific mission objectives. Moreover, AUV control systems must be able to operate autonomously, without requiring constant human input, and adapt to changing environmental conditions in real-time [1,3]. A robust algorithm can provide estimation of linear and angular position and velocities of the vehicle (navigation), process navigation/ inertial reference trajectory data and output set-points for the vehicle's velocity and altitude (guidance), and generate thruster signals that are required to drive the actual velocity and altitude of the vehicle to the value commanded by the guidance schemes (control) [5,6].

The motion of an AUV is governed by the laws of physics, which can be expressed mathematically through the equations of motion. Newton-Euler (NE) and Lagrange-Euler (LE) formulations are two common approaches for deriving the equations of motion for AUVs [5,7]. For the purpose of this project, the Newton-Euler approach was used due to its computational efficiency. In this method, the dynamics of a system are represented by a set of force and moment balance equations, which relate the external forces and moments acting on the system to its motion and acceleration. The equations of motion derived by the Newton-Euler method are in terms of linear and angular velocities and accelerations of the rigid body.

The objective of this thesis was to develop a precise dynamic model and suitable control schemes for HM-AUVs to be capable of independently achieving full controllable 6-DoF (x, y, z, roll, pitch, yaw) motion, allowing them to have high maneuverability and navigate in confined spaces subject to disturbances. One of the challenges in controlling the vehicle is due to the coupling effects of its motion; for instance, controlling the vehicle's lateral motion produces a significant yawing momentum which can be problematic for controlling the vehicle and one of the challenges is to design the dynamic model that can address most of the couplings and trying to decouple them. In this project, the full dynamic model of the vehicle was developed using Newton-Euler approach and considering different coupling effects so the vehicle can perform sophisticated maneuvers. A simulated model of the HM-AUV and its control system

was then developed in Simulink environment to analyze and verify the behavior of the vehicle completing logarithmic spiral trajectory. A set of six PID controllers were used for each degree of freedom to help for the desire performance of the vehicle. The vehicle used for this project is a highly maneuverable autonomous underwater vehicle (HM-AUV) which is being developed in Unmanned Vehicle Robotarium laboratory at the University of Calgary by Dr. Alex Ramirez-Serrano. Due to its configuration, HM-AUV is capable of performing acrobatic maneuvers in highly confines spaces. The vehicle has 3 tilting-thruster configuration (one thruster at the tail of the vehicle and two thrusters on left and right sides of the main hull, each being attached to the body by a serial servo motor allowing them to rotate 360 degrees along their tilting axes.) as can be seen in figure 1.

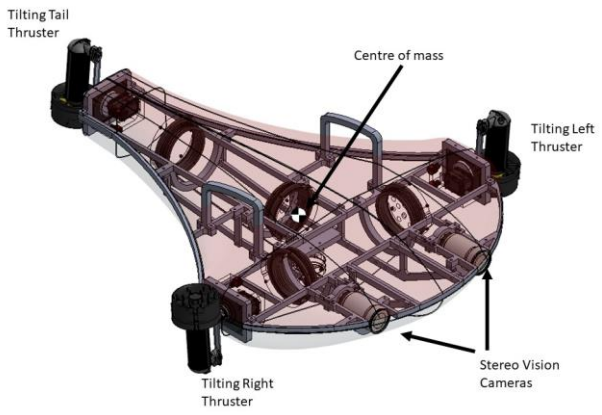


Figure1: The Highly Maneuverable Autonomous Underwater Vehicle (HM-AUV)

Each thruster can produce thrust vectoring force in different directions by dynamically tilting along its thrust plane to generate thrust force at multiple angles, allowing it to control its independent motion in all degrees of freedom.

**Dynamic Model Development**

In this section, the HM-AUV's dynamic model will be developed. Different external forces such as Coriolis force, drag force and several hydrodynamic forces and moments will be analyzed and introduced to the dynamic model.

Prior to developing the dynamic model of the HM-AUV, it is essential to define the terms used to describe its motion. Table 1 displays some of the parameter names used in this section. The forward and reverse motion of the vehicle (in x direction) is known as the Surge, its lateral movement (in y direction) is referred to as Sway, and its ascending and descending movement (in z direction) is referred to as Heave. The angular movements of an underwater vehicle (about x, y and z axis) are denoted by the terms Roll, Pitch, and Yaw. For a full description of all variables and parameters used in this paper, please refer to the appendix.

Table 1: Common notations for the motion of the HM-AUV

| Nautical Term | Position/Euler Angles (EF) | Force/Moment (BF) | Translational/Angular Velocity (BF) |
|---|---|---|---|
| Surge | x | X | u |
| Sway | y | Y | v |
| Heave | z | Z | w |
| Roll | φ | K | p |
| Pitch | θ | M | q |
| Yaw | ψ | N | r |

In the development of a dynamic model for an AUV, it is important to define the coordinate systems that will be used to describe the vehicle's motion. There are two commonly used coordinate systems in AUV modeling which are body frame and the inertial reference frame (earth). The body frame is a coordinate system that is attached to the AUV itself, with the origin located at the center of mass of the vehicle and axis being attached to it as can be seen in figure 2. In the body frame, the motion of the AUV is described in terms of its own orientation and velocity. The inertial reference frame is a coordinate system that is fixed to the earth, with the origin located at a fixed point on the earth's surface. In the inertial reference frame, the motion of the AUV is described in terms of its position and velocity relative to the earth. When developing a dynamic model for an AUV, it is generally easier to describe the vehicle's motion in the body frame, rather than the inertial reference frame. This is because the AUV is designed to maneuver and change

its orientation in the water, and its motion is often influenced by external forces, such as currents and waves. By describing the motion in the body frame, the model can take these factors into account and accurately predict the behavior of the vehicle [2,8].

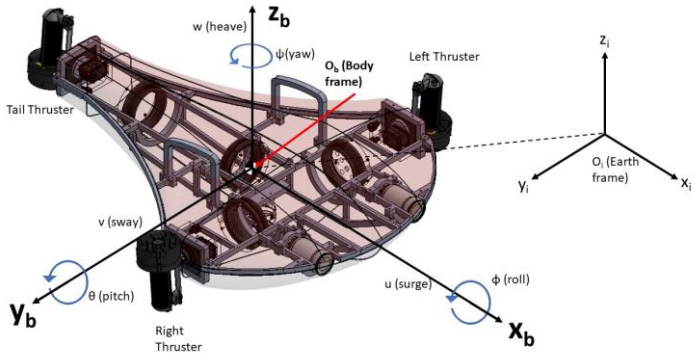


Figure 2: Representation of the inertial and body frames

To drive the specific transformation matrix for moving a dynamic model from the Earth frame to the body frame, first the coordinate frames were explicitly defined. The position and orientation of the vehicle with respect to the inertial frame is being defined as:

$$\eta_1 = [x, y, z]^T; \quad \eta_2 = [\varphi, \theta, \psi]^T \tag{1}$$

while the position and orientation of the vehicle with respect to its body frame is:

$$v_1 = [u, v, w]^T; \quad v_2 = [p, q, r]^T \tag{2}$$

The transformation matrix is made up of three rotation matrices, one for each axis as illustrated in Eq.3. The rotation matrices are determined by the angles of rotation about each axis and for the x, y, and z axes are given by:

$$R_{x(\varphi)} = \begin{pmatrix} 1 & 0 & 0 \\ 0 & \cos(\varphi) & -\sin(\varphi) \\ 0 & \sin(\varphi) & \cos(\varphi) \end{pmatrix} \quad , \quad R_{y(\theta)} = \begin{pmatrix} \cos(\theta) & 0 & \sin(\theta) \\ 0 & 1 & 0 \\ -\sin(\theta) & 0 & \cos(\theta) \end{pmatrix}$$

$$R_{z(\psi)} = \begin{pmatrix} \cos(\psi) & -\sin(\psi) & 0 \\ \sin(\psi) & \cos(\psi) & 0 \\ 0 & 0 & 1 \end{pmatrix} \quad (3)$$

Combining the matrices together, gives the following transformation matrix (being called Jacobian matrix) for the transformation of rotational velocities between the frames:

$$J_{2(\eta_2)} = \begin{pmatrix} \cos(\psi)\cos(\theta) & -\sin(\psi)\cos(\varphi) + \cos(\psi)\sin(\theta)\sin(\varphi) & \sin(\psi)\sin(\varphi) + \cos(\psi)\sin(\theta)\cos(\varphi) \\ \sin(\psi)\cos(\theta) & \cos(\psi)\cos(\varphi) + \sin(\psi)\sin(\theta)\sin(\varphi) & -\cos(\psi)\sin(\varphi) + \sin(\psi)\sin(\theta)\cos(\varphi) \\ -\sin(\theta) & \cos(\theta)\sin(\varphi) & \cos(\theta)\cos(\varphi) \end{pmatrix} \quad (4)$$

And the relationship between rotational velocities between inertial and body frame will be:

$$\eta 2 = J2(\eta 2)v2 \rightarrow \begin{matrix} \dot{\varphi} \\ \dot{\theta} \\ \dot{\psi} \end{matrix} = J2(\eta 2) \begin{matrix} p \\ q \\ r \end{matrix} \quad (5)$$

Next it is required to determine the translation vector which represents the position of the origin of the body frame in the Earth frame and by applying the same rules it results in the following transformation matrix Eq. 6 for the translational velocity:

$$\eta 1 = J1(\eta 1)v1 \rightarrow \begin{matrix} \dot{x} \\ \dot{y} \\ \dot{z} \end{matrix} = J1(\eta 1) \begin{matrix} u \\ v \\ w \end{matrix} \quad \text{, where: } J1(\eta 1) = \begin{pmatrix} 1 & \sin(\varphi)\tan(\theta) & \cos(\varphi)\tan(\theta) \\ 0 & \cos(\varphi) & -\sin(\varphi) \\ 0 & \sin(\varphi)/\cos(\theta) & \cos(\varphi)/\cos(\theta) \end{pmatrix} \quad (6)$$

With introducing Eq. 4 and 6, we can transform any rotational and translational velocities between the two defined frame [2,4].

The motion of the HM-AUV can be described by a set of differential equations that model the movement and orientation of the vehicle and the equations of motion can be derived using Newton-Euler equations [9,10]. The equation of motion will be expressed as $M\dot{v} + C(v)v + D(v)v + g = \tau_c$, (7) where M, C, D, and g are matrices and vectors that represent the mass, Coriolis, drag and gravitational forces

acting on the HM-AUV, respectively, v is the velocity of the AUV, and $\tau_c$ being the produced vehicle's thrust force. After defining the coordinate systems (body and inertial frames), the corresponding Jacobian Matrix and motion variables (position, velocity, acceleration, orientation, angular velocity, and angular acceleration), the Newton's second law of motion Eq. 8 was then applied to the HM-AUV which mathematically, can be written as:

$$F = M\dot{v} \tag{8}$$

Where F is all the forces acting on the vehicle, M is its corresponding mass and $v$ is its translational and angular velocities being $v = [u, v, w, p, q, r]^T$.

Next, the Euler equation Eq.9 was used to consider the effects of the HM-AUV's rotation on its motion. The Euler equation relates the rate of change of angular momentum to the torque acting on a rigid body. In vector form, the Euler equation is:

$$I\dot{\omega} + \omega \times (I\omega) = \tau \tag{9}$$

Where I is the moment of inertia matrix, $\omega$ is the angular velocity vector, and $\tau$ is the torque vector.

By taking the time derivative of this equation and substituting in the expression for angular acceleration ($\dot{\omega}$), an equation relating the torque to the rate of change of angular velocity was obtained. Using this equation and the principle of conservation of angular momentum, an expression for the Coriolis matrix was derived. The Coriolis force arises due to the rotation of the vehicle and the motion of the fluid around it. The Coriolis effect can be broken down into two parts: the Coriolis force due to the added mass and the Coriolis force due to the rigid body. The Coriolis force due to the added mass arises due to the interaction between the AUV and the surrounding fluid and is caused by the acceleration of the fluid around the AUV. This force depends on the AUV's velocity and the rate of change of its angular velocity as can be seen in Eq. 10. The Coriolis force due to the rigid body is also known as the Coriolis centripetal force or the centrifugal force. It arises due to the rotation of the AUV about its center of mass and depends on the angular velocity of the AUV.

$C_{RB}(v)$=

$$\begin{pmatrix} 0 & 0 & 0 & m(y_g q + z_g r) & -m(x_g q - w) & -m(x_g r + v) \\ 0 & 0 & 0 & -m(y_g q + w) & m(z_g r + x_g p) & -m(y_g r - u) \\ 0 & 0 & 0 & -m(z_g p - v) & -m(z_g q + u) & m(x_g p + y_g q) \\ 0 & -I_{yz}q - I_{xz}p + I_z r & I_{yz}r + I_{xy}p - I_y q & 0 & 0 & 0 \\ I_{yz}q + I_{xz}p - I_z r & 0 & -I_{xz}r - I_{xy}q + I_x p & 0 & 0 & 0 \\ -I_{yz}r - I_{xy}p + I_y q & I_{xz}r + I_{xy}q - I_x p & 0 & 0 & 0 & 0 \end{pmatrix}$$

$$C_{ADD}(v) = \begin{pmatrix} 0 & 0 & 0 & 0 & -b_3 & b_2 \\ 0 & 0 & 0 & b_3 & 0 & -b_1 \\ 0 & 0 & 0 & -b_2 & b_1 & 0 \\ 0 & -b_3 & b_2 & 0 & -a_3 & a_2 \\ b_3 & 0 & -b_1 & a_3 & 0 & -a_1 \\ -b_2 & b_1 & 0 & -a_2 & a_1 & 0 \end{pmatrix}$$ where:

$$b_1 = X_{\dot{u}}u + X_{\dot{v}}v + X_{\dot{w}}w + X_{\dot{p}}p + X_{\dot{q}}q + X_{\dot{r}}r$$
$$b_2 = Y_{\dot{u}}u + Y_{\dot{v}}v + Y_{\dot{w}}w + Y_{\dot{p}}p + Y_{\dot{q}}q + Y_{\dot{r}}r$$
$$b_3 = Z_{\dot{u}}u + Z_{\dot{v}}v + Z_{\dot{w}}w + Z_{\dot{p}}p + Z_{\dot{q}}q + Z_{\dot{r}}r$$
$$a_1 = K_{\dot{u}}u + K_{\dot{v}}v + K_{\dot{w}}w + K_{\dot{p}}p + K_{\dot{q}}q + K_{\dot{r}}r$$
$$a_2 = M_{\dot{u}}u + M_{\dot{v}}v + M_{\dot{w}}w + M_{\dot{p}}p + M_{\dot{q}}q + M_{\dot{r}}r$$
$$a_3 = N_{\dot{u}}u + N_{\dot{v}}v + N_{\dot{w}}w + N_{\dot{p}}p + N_{\dot{q}}q + N_{\dot{r}}r$$

(10)

Similarly, to account for the effect of the surrounding fluid on the HM-AUV's motion, the drag matrix was derived using Eq. 11:

$$F_{Drag} = \frac{1}{2}\rho v^2 A C_D \quad (11)$$

Where $\rho$ is the water's density, v is the vehicle's velocity, A is its frontal area, and $C_D$ is the drag coefficient.

The drag matrix, D(v), Eq.12 accounts for the effect of fluid viscosity and friction on the AUV's motion. It is also a function of the AUV's velocity and is typically obtained by conducting experiments or simulations to determine the drag coefficients.

$$D(v) = -diag(X_u + X_{u|u}|u|, Y_v + Y_{v|v}|v|, Z_w + Z_{w|w}|w|, K_p + K_{p|p}|p|, M_q + M_{q|q}|q|, N_r + N_{r|r}|r|) \quad (12)$$

Finally, the mass matrix M was identified as in Eq.13. The mass matrix describes the added mass and rigid body mass of the AUV. The added mass accounts for the additional mass of fluid that is

displaced by the AUV as it moves through water while the rigid body mass accounts for the mass of the AUV itself.

$$M_{RB} = \begin{pmatrix} m & 0 & 0 & 0 & mz_g & -my_g \\ 0 & m & 0 & -mz_g & 0 & mx_g \\ 0 & 0 & m & my_g & -mx_g & 0 \\ 0 & -mz_g & my_g & I_x & -I_{xy} & -I_{xz} \\ mz_g & 0 & -mx_g & -I_{xy} & I_y & -I_{yz} \\ -my_g & mx_g & 0 & -I_{xz} & -I_{yz} & I_z \end{pmatrix}, M_{ADD} = - \begin{pmatrix} X_{\dot{u}} & X_{\dot{v}} & X_{\dot{w}} & X_{\dot{p}} & X_{\dot{q}} & X_{\dot{r}} \\ Y_{\dot{u}} & Y_{\dot{v}} & Y_{\dot{w}} & Y_{\dot{p}} & Y_{\dot{q}} & Y_{\dot{r}} \\ Z_{\dot{u}} & Z_{\dot{v}} & Z_{\dot{w}} & Z_{\dot{p}} & Z_{\dot{q}} & Z_{\dot{r}} \\ K_{\dot{u}} & K_{\dot{v}} & K_{\dot{w}} & K_{\dot{p}} & K_{\dot{q}} & K_{\dot{r}} \\ M_{\dot{u}} & M_{\dot{v}} & M_{\dot{w}} & M_{\dot{p}} & M_{\dot{q}} & M_{\dot{r}} \\ N_{\dot{u}} & N_{\dot{v}} & N_{\dot{w}} & N_{\dot{p}} & N_{\dot{q}} & N_{\dot{r}} \end{pmatrix} \quad (13)$$

Furthermore, Eq. 7 account for the force of gravity; however, since HM-AUV is designed to be neutrally buoyant, meaning that it is able to float at a constant depth without sinking or rising and the vehicle's weight is equal to the buoyant force exerted on it by the surrounding water, the gravitational forces and the buoyant forces cancel each other out and these forces can be removed from the equations of motion. Putting it all together, the equation of motion for the HM-AUV was developed as Eq.14:

$$M\dot{v} + C(v)v + D(v)v = \tau_c \quad (14)$$

Where $M = M_{RB} + M_{ADD}$ and $C = C_{RB} + C_{ADD}$.

**Control Section**

In this section the required thrust force equations corresponding to each thruster will be developed with their corresponding tilting angles, while considering the coupling effects. There will be a brief introduction to controllers and the use of PID controller for the derived model.

One of the key components of an AUV is its controller, which is responsible for regulating the vehicle's motion and ensuring that it performs its assigned task accurately. The controller of an AUV is crucial in regulating the vehicle's motion and ensuring accurate performance. A PID controller, consisting of proportional, integral, and derivative components, is commonly used in industrial automation and control systems. It can handle various input signals and is easily tunable. To reach a desired position and orientation, the controller will manipulate forces based on the current position and goal pose. A suitable algorithm in

MATLAB software will calculate control inputs, including force and thruster orientation, for each of the six degrees of freedom using a PID controller [2,4].

First, the actual/ initial position and orientation of the vehicle $(x_0, y_0, z_0, \varphi_0, \theta_0, \psi_0)$ and the initial translational and angular velocities $(u_0, v_0, w_0, \mathrm{p}_0, \mathrm{q}_0, \mathrm{r}_0)$ w.r.t inertial coordinate is given to the PID control system as the initial condition of the vehicle and the corresponding initial matrices $\eta_0$, $C(v_0), and\ D(v_0)$ is calculated. As the nest step, the current η and desired pre-programed $\eta_d$ set points of the vehicle in inertial frame for its motion is compared and the error (Eq.15) and its derivative is determined as follows:

$$e = \eta_d - \eta \ \longrightarrow\ \dot{e} = -\dot{\eta} = -J(\eta)\upsilon \qquad where\ J(\eta) = [J1(\eta), J2(\eta)]^T \tag{15}$$

The error matrix will then be inputted to the controller and the PID control rule (Eq. 16) will be applied.

$$\tau_c = \mathrm{J}(\eta)^T (K_p e + K_i \int e + K_D \dot{e}) \tag{16}$$

Where $K_p$, $K_i$, and $K_D$ are proportional, integral, and derivative gains, respectively and their values were defined using tuning tool in Simulink, and $\tau_c$ is the control input corresponds to the forces acting on HM-AUV and is $\tau_c = [X, Y, Z, K, M, N]^T$.

An individual PID controller was applied to each DOF. These controllers then output the required translational and rotational forces [X, Y, Z, K, M, N] and in the following, based on the calculated control matrix, the required directional thrust force components and tilting angles will be calculated from the controllers' outputs. Due to the specific configuration of HM-AUV, the right and left thrusters can contribute to the motion in x and z direction while tail thruster can contribute to the motion in y and z direction and with this combination, $X, Y, and\ Z$ can be determined based on the forced produced by each component of each thruster (Eq. 17). Moreover, the moments acting on the HM-AUV $(K, M, and\ M)$ can also be calculated using the fact that due to the configuration only the right and left thrusters contribute to the rolling and yawing motion, while all the three thrusters contribute to the pitching motion. moreover, it

had to be considered that the sum of the moments in each direction should cancel out each other. Using the preceding statements, the components of forces produced by each thruster was calculated (Eq. 19), where the right, left and tail thrusters have their corresponding indices of i=1, 2, and 3, respectively. Please note that the following equations can have many solutions; however, by considering the configuration and the efficiency of the vehicle, the solutions in front of each equation were considered.

$$\begin{gathered} f_{1x} + f_{2x} = X \longrightarrow f_{1x} = f_{2x} = \frac{X}{2} \\ f_{3y} = Y \\ f_{1z} + f_{2z} + f_{3z} = Z \longrightarrow f_{1z} = f_{2z} = f_{3z} = \frac{Z}{3} \\ f_{1z} * w - f_{2z} * w = K \longrightarrow f_{1roll} = f_{2roll} = \frac{K}{w} \\ f_{1z} * 2l + f_{2z} * 2l - f_{3z} * l = M \longrightarrow f_{1pitch} = f_{2pitch} = \frac{M}{2l} \ , \ f_{3pitch} = \frac{M}{l} \\ f_{1x} * 2xr - f_{2x} * 2xl = N \longrightarrow f_{1yaw} = f_{2yaw} = \frac{N}{2x} \end{gathered} \tag{17}$$

Due to the configuration of the HM-AUV, there is a significant yawing momentum while the vehicle tries to have lateral motion (sway) and in order to decouple and cancel the effect, the left and right thrusters have to produce momentum in the opposite direction as follows:

$$f_{2addsway} * 2xl - f_{1addsway} * 2xr = Y \longrightarrow f_{1addsway} = f_{2addsway} = \frac{Y}{2x} \tag{18}$$

Considering the coupling effects and deriving the above equations for each degree of freedom, the total force required to be generated by each thruster can then be determined (Eq.19):

$$\begin{gathered} f_1 = \sqrt{f_{1x}^2 + f_{1yaw}^2 - f_{1addsway}^2 + f_{1z}^2 + f_{1roll}^2 + f_{1pitch}^2} \longrightarrow f_1 = \sqrt{\left(\frac{X}{2}\right)^2 + \left(\frac{N}{2x}\right)^2 - \left(\frac{Y}{2x}\right)^2 + \left(\frac{Z}{3}\right)^2 + \left(\frac{K}{w}\right)^2 + \left(\frac{M}{2l}\right)^2} \\ f_2 = \sqrt{f_{2x}^2 - f_{2yaw}^2 + f_{2addsway}^2 + f_{2z}^2 - f_{2roll}^2 + f_{2pitch}^2} \longrightarrow f_2 = \sqrt{\left(\frac{X}{2}\right)^2 - \left(\frac{N}{2x}\right)^2 + \left(\frac{Y}{2x}\right)^2 + \left(\frac{Z}{3}\right)^2 - \left(\frac{K}{w}\right)^2 + \left(\frac{M}{2l}\right)^2} \\ f_3 = \sqrt{f_{3y}^2 + f_{3z}^2 - f_{3pitch}^2} \longrightarrow f_3 = \sqrt{Y^2 + \left(\frac{Z}{3}\right)^2 - \left(\frac{M}{l}\right)^2} \end{gathered} \tag{19}$$

After calculating the sum of each of the directional components, the required tilting angle for each thruster was determined using inverse trigonometric functions (Eq. 20).

$$\theta_1 = atan2\left(\frac{f_{1z}+f_{1roll}+f_{1pitch}}{f_{1x}+f_{1yaw}-f_{1addsway}}\right) \longrightarrow \theta_1 = atan2\left(\frac{\frac{Z}{3}+\frac{K}{w}+\frac{M}{2l}}{\frac{X}{2}+\frac{N}{2x}-\frac{Y}{2x}}\right)$$
$$\theta_2 = atan2\left(\frac{f_{2z}-f_{2roll}+f_{2pitch}}{f_{2x}-f_{2yaw}+f_{2addsway}}\right) \longrightarrow \theta_2 = atan2\left(\frac{\frac{Z}{3}-\frac{K}{w}+\frac{M}{2l}}{\frac{X}{2}-\frac{N}{2x}+\frac{Y}{2x}}\right) \quad (20)$$
$$\theta_3 = atan2\left(\frac{f_{3z}-f_{3pitch}}{f_{3y}}\right) \longrightarrow \theta_3 = atan2\left(\frac{\frac{Z}{3}-\frac{M}{l}}{Y}\right)$$

Having calculated all the components, the dynamic equation of HM-AUV is:

$$\dot{v} = -M^{-1}(C(v_0)v_0 + D(v_0)v_0) + M^{-1}\tau_{c0} \quad (21)$$

And taking the integral of $\dot{v}$, the required translational and angular velocities for the vehicle to follow the desired path can be determined $(u, v, w, p, q, r)$. Using Jacobian matrix, the determined velocities in the body frame transforms to the inertial frame $(\dot{x}, \dot{y}, \dot{z}, \dot{\varphi}, \dot{\theta}, \dot{\psi})$ which are the translational and angular velocity in the Earth frame and by taking their integral the updated current position/ orientation of the vehicle can be found $(x, y, z, \varphi, \theta, \psi)$. The new position/ orientation matrix will once again being compared to the desired ones and the error matrix will be calculated and the cycle continuous until the vehicle finishes its mission.

**Results**

In this section, the set-up for the developed simulation framework used to test, analyze, and characterize the proposed controller is described. The motion of the HM-AUV will be simulated for a complex logarithmic spiral trajectory over 80 seconds and it will be shown that with proposed controller and dynamic model and based on the specific configuration of the HM-AUV with 3 thrusters producing variable thrust vectoring, the vehicle has high maneuverability. Finally, the breakdown of motion including the rotation (roll, pitch and yaw) and translation (sway, heave and surge) motions will be tested to analyze the response of the HM-AUV performing acrobatic 3D movements.

A simulation framework developed around MATLABR2022b, and Simulink (for model-based design and simulation of the dynamic system). A detailed dynamic model of the vehicle was imported in MATLAB and was defined in each specific block of Simulink as shown in figure 3.

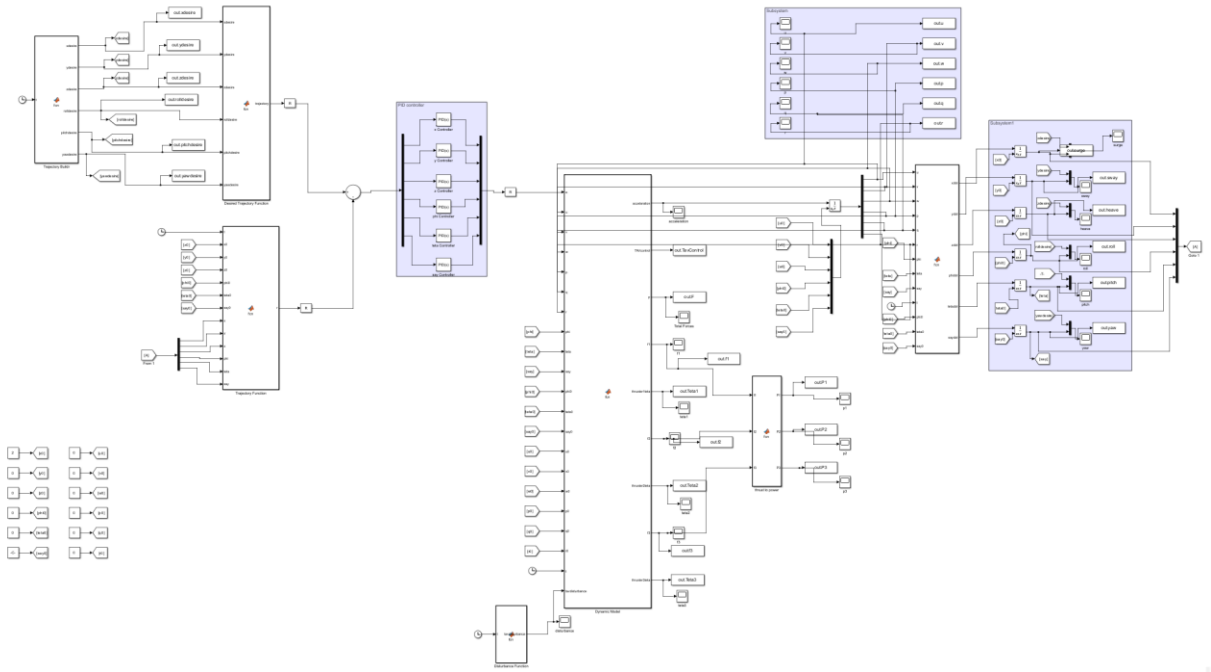

Figure 3: Simulation environment

**Spiral trajectory:** For testing the high maneuverability of the vehicle, the complex Logarithmic spiral trajectory was chosen which requires the simultaneous control of all six degrees of freedom. The equations of the trajectory were defined as in Eq. 22, where $\omega = \frac{\pi}{10}$.

$$x_{Desire} = e^{-0.01t}\cos(\omega t), \quad y_{Desire} = e^{-0.01t}\sin(\omega t), \quad z_{Desire} = 0.25t \tag{22}$$

$$\varphi_{Desire} = \pi \sin(\omega t), \quad \theta_{Desire} = \frac{\pi}{3}\cos(\omega t), \quad \psi_{Desire} = 0.25t$$

The comparison between the desired and simulated 3D trajectory as well as the breakdown for each translational motion (surge, sway, and heave) is shown in figure 4 and 5.

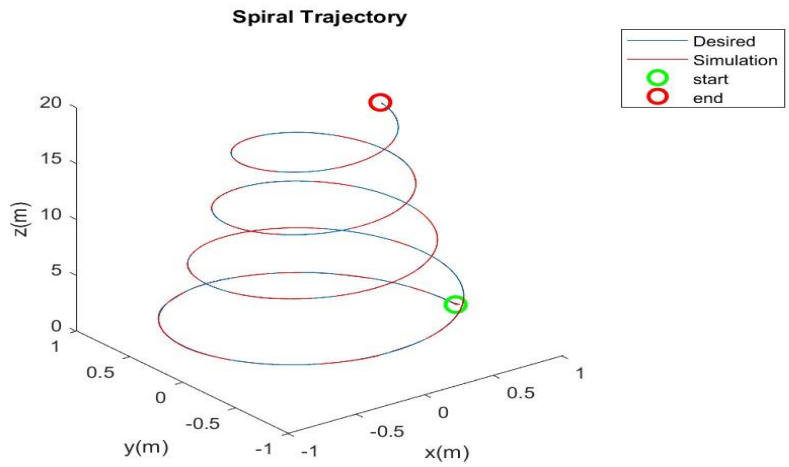


Figure 4: Comparison between the desired and simulated motion of HM-AUV following Logarithmic Spiral Trajectory

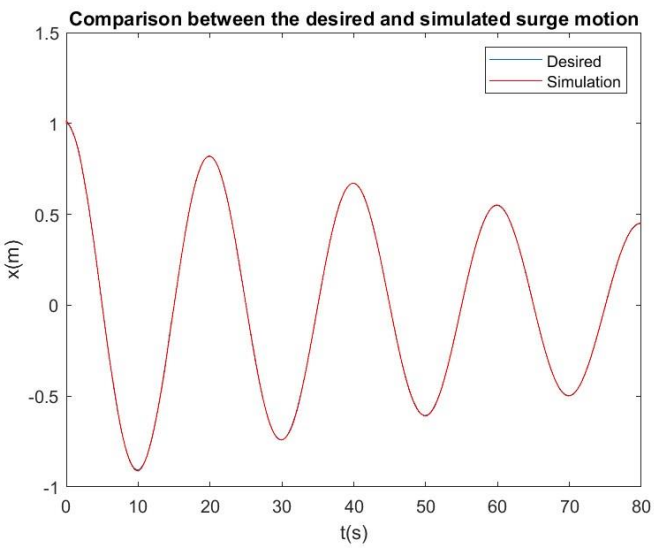


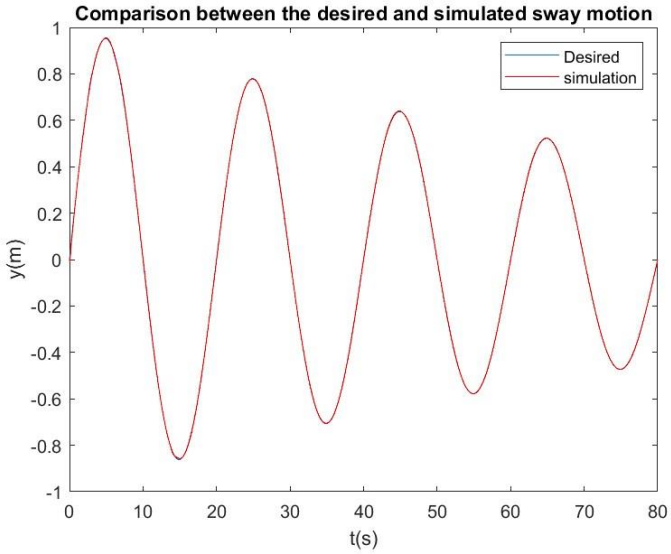

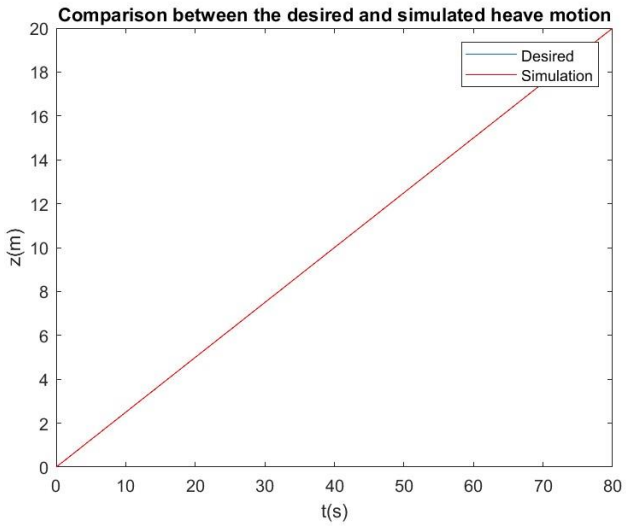


Figure 5: Comparison between the desired and simulated translational motion of HM-AUV following Logarithmic Spiral Trajectory; Surge motion on left, sway motion on right, and heave motion on the bottom

Figures 4 and 5 show that the proposed dynamic model and controller for HM-AUV was successful at giving the vehicle a fully autonomy over its 6 DOFs as there is zero deviation from the desired (blue) and simulated (red) spiral trajectories. Moreover, the breakdown of comparison between desired and simulated translational (surge, sway, and heave) motion also show the minimum (zero) deviation and error between desired (blue) and simulated (red) motions. In addition, the breakdown of rotational motion (roll, pitch and yaw) is shown in figure 6:

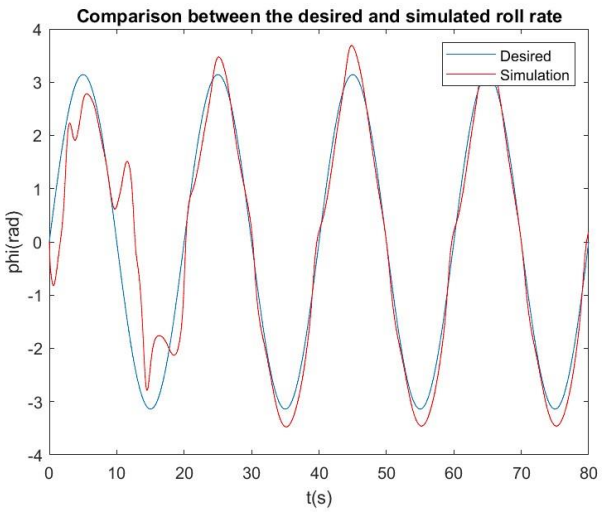


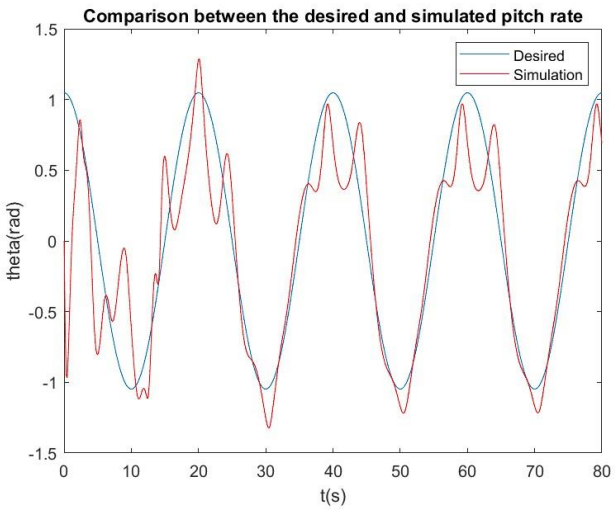

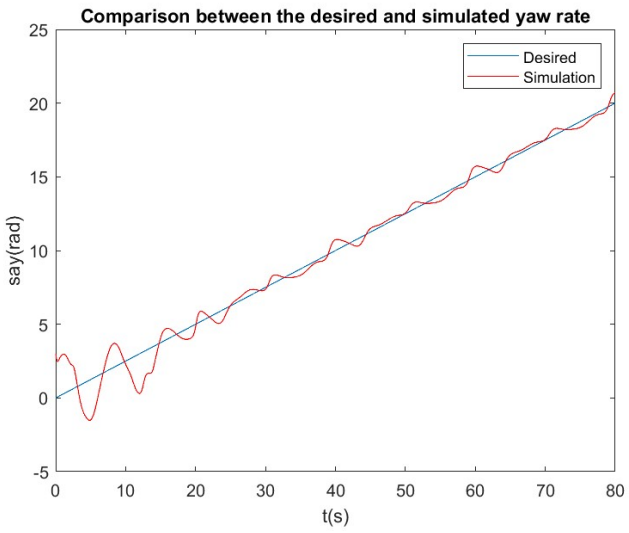


Figure 6: Comparison between desired and simulated rotational motions of HM-AUV following Logarithmic Spiral Trajectory; roll motion on left, pitch motion on right, and yaw motion on the bottom

Figure 6 shows that the vehicle was also successful at following the overall rotational motion and the coupling effects tried to be minimized by the proposed dynamic model. While there is still some deviation from the desired and simulated rotational motions, it is not significant (the overall error is less than %5), they were attributed to the coupling effects and complexity of the dynamic of the vehicle, which were deemed to be too small to be neglected over the time. For the logarithmic spiral trajectory, it can be observed that most of the deviations occurred for the pitch motion which tried to be minimized by considering the momentum term in sway motion from the left and right thrusters (Eq.18).

**Conclusion and Future Work**

The aim of this project was to enhance the control of an HM-AUV to achieve full autonomy over its 6 degrees of freedom and perform complex acrobatic maneuvers in confined spaces. The results demonstrated that the developed dynamic model and control system were highly effective in achieving such complex trajectories, with slight errors and overshoot that were considered insignificant given the vehicle's dynamic complexity. The analysis of surge, sway, and heave motion, as well as the rotational motions, provided a comprehensive understanding of the HM-AUV's performance following logarithmic trajectory.

This study has important implications for the development of more advanced underwater vehicles and control systems. Future work includes experimental testing in real-world environments to verify the accuracy of the simulations, and the exploration of more advanced controllers such MPCs to study the vehicle's behavior under environmental disturbances.

**Appendices:**

List of Abbreviations and Symbols

| **Acronym** | **Definition** |
|---|---|
| AUV | Autonomous Underwater Vehicle |
| DOF | Degree of Freedom |
| GPS | Global Positioning System |
| HM-AUV | Highly Maneuverable Autonomous Underwater Vehicle |
| PID | Proportional Integral Derivative |
| w.r.t. | With Respect to |
| MPC | Model Predictive Controller |

| **Symbols** | **Definition** |
|---|---|
| $\eta 1$ | Position vector of the vehicle w.r.t. inertial reference frame |
| $\eta 2$ | Position vector of the vehicle w.r.t. body frame |
| $v1$ | Translational velocity vector of the vehicle w.r.t. body frame |
| $v2$ | Rotational velocity vector of the vehicle w.r.t. body frame |
| $\rho$ | Density of Water |
| $M_{RB}$ | Rigid body mass matrix |
| $M_{Add}$ | Added mass matrix |
| $C_{RB}$ | Rigid body Coriolis matrix |
| $C_{ADD}$ | Added Coriolis matrix |
| D | Drag force matrix |
| $C_D$ | Drag force coefficient |

| | |
|---|---|
| X, Y, Z | Forces acting on HM-AUV along the x, y and z directions respectively |
| K, M, N | Moments acting on HM-AUV along the x, y and z directions respectively |
| | Distance from left, right and tail thrusters to the CoG in the x-axis |
| x, y, z | Translational position along the x, y and z directions w.r.t. the inertial frame |
| u, v, w | Translational velocities along the x, y and z directions w.r.t. the body frame |
| φ, θ, ψ | Angular position along the x, y and z directions w.r.t. the inertial frame |
| p, q, r | Angular velocities about the x, y and z directions w.r.t. the body frame |
| R | Cosine Transformation Matrix |
| $J1(\eta 1)$ | Jacobian matrix to convert translational velocities between inertial and body frames |
| $J2(\eta 2)$ | Jacobian matrix to convert angular velocities between inertial and body frames |
| $I_{xx}, I_{xy}, I_{xz}$ | Moments of inertia around x-axis |
| $I_{yx}, I_{yy}, I_{yz}$ | Moments of inertia around y-axis |
| $I_{zx}, I_{zy}, I_{zz}$ | Moments of inertia around z-axis |

$X_{\dot{u}}, X_{\dot{v}}, X_{\dot{w},}\ X_{\dot{p}}, X_{\dot{q}}, X_{\dot{r}}$ The forces in x direction resulted from added due to surge, sway, heave, roll, pitch, and yaw acceleration, respectively

$Y_{\dot{u}}, Y_{\dot{v}}, Y_{\dot{w},}\ Y_{\dot{p}}, Y_{\dot{q}}, Y_{\dot{r}}$ The forces in y direction resulted from added due to surge, sway, heave, roll, pitch, and yaw acceleration, respectively

$Z_{\dot{u}}, Z_{\dot{v}}, Z_{\dot{w},}\ Z_{\dot{p}}, Z_{\dot{q}}, Z_{\dot{r}}$ The forces in z direction resulted from added due to surge, sway, heave, roll, pitch, and yaw acceleration, respectively

$K_{\dot{u}}, K_{\dot{v}}, K_{\dot{w},}\ K_{\dot{p}}, K_{\dot{q}}, K_{\dot{r}}$ The moments in x direction resulted from added due to surge, sway, heave, roll, pitch, and yaw acceleration, respectively

$M_{\dot{u}}, M_{\dot{v}}, M_{\dot{w}}, M_{\dot{p}}, M_{\dot{q}}, M_{\dot{r}}$ The moments in y direction resulted from added due to surge, sway, heave, roll, pitch, and yaw acceleration, respectively

$N_{\dot{u}}, N_{\dot{v}}, N_{\dot{w}}, N_{\dot{p}}, N_{\dot{q}}, N_{\dot{r}}$ The moments in z direction resulted from added due to surge, sway, heave, roll, pitch, and yaw acceleration, respectively

| | |
|---|---|
| $X_u$ | First order hydrodynamic force in x direction due to surge motion |
| $Y_v$ | First order hydrodynamic force in y direction due to sway motion |
| $Z_w$ | First order hydrodynamic force in z direction due to heave motion |
| $K_p$ | First order hydrodynamic force in x direction due to roll |
| $M_q$ | First order hydrodynamic force in y direction due to pitch |
| $N_r$ | First order hydrodynamic force in z direction due to yaw |
| $X_{u\|u}$ | Second order hydrodynamic force in x direction due to surge motion |
| $Y_{v\|v}$ | Second order hydrodynamic force in y direction due to sway motion |
| $Z_{w\|w}$ | Second order hydrodynamic force in z direction due to heave motion |
| $K_{p\|p}$ | Second order hydrodynamic force in x direction due to roll |
| $M_{q\|q}$ | Second order hydrodynamic force in y direction due to pitch |
| $N_{r\|r}$ | Second order hydrodynamic force in z direction due to yaw |
| $e$ | Error vector |
| $K_p$ | PID proportional term |
| $K_i$ | PID integral term |

$K_D$ PID derivative term

Table 2: HM-AUV's Parameters

| Parameter | Value |
|---|---|
| Vehicle's Weight (kg) | 12.437 |
| Moments of Inertia (kg∗ $m^2$) | $I_{xx} = 6741.44, I_{xy} = 1906.18, I_{xz} = 3580.59$<br>$I_{yx} = 1906.18, I_{yy} = 8454.36, I_{yz} = 2508.82$<br>$I_{zx} = 3580.59, I_{zy} = 2508.82, I_{zz} = 4399.80$ |
| Hydrodynamic Coefficients | $X_{\dot{u}} = -38.4, Y_{\dot{v}} = -74.81, Z_{\dot{w}} = -11.47,$<br>$K_{\dot{p}} = -3.65, M_{\dot{q}} = -5.72, N_{\dot{r}} = -4.84$<br>$X_{u\|u} = -34.55, Y_{v\|v} = -104.40,$<br>$Z_{w\|w} = -146.50, K_{p\|p} = 0.71, M_{q\|q} = -5.73$<br>$N_{r\|r} = -4.01$<br>The rest of hydrodynamic parameters are zero. |
| Length (m) | L=$x_r$+$x_l$=0.135+0.135=0.885 |
| Width (m) | W=$y_r$=$y_l$=0.45 |
| Height (m) | $z_g$=0.12 |

References

[1] S.A. Wadoo, P. Kachroo, Autonomous Underwater Vehicles, Modeling, Control Design, and Simulation, 2011.

[2] A. Kadkhodaei, R.H. Ghasemi, Representation of New Variable Thrust Vector Underwater Robotic Platform for Complex Trajectory Tracking, J. Eur. Des Systèmes Autom. 54 (2021) 411–421. https://doi.org/10.18280/jesa.540304.

[3] L. Li, J. Li, G. Li, Research on autonomous underwater vehicle control technology: A review, J. Mar. Sci. Eng. 4 (2016).

[4] J.A.G. Rodriguez, Control for a Highly Maneuverable Autonomous Underwater Vehicle, University of Calgary, M.Sc. Thesis, 2020.

[5] T.I. Fossen, Handbook of Marine Craft Hydrodynamics and Motion Control, 2011.

[6] D. Fryxell, P. Oliveira, A. Pascoal, C. Silvestre, I. Kaminer, Navigation, Guidance and Control of AUVs: An Application to the MARIUS Vehicle, IFAC Proc. Vol. 28 (1995) 35–42.

[7] P. Tsiotras, T. Lee, J.-J. Slotine, Nonlinear control of underwater vehicles: a Lyapunov-based approach, in: Proc. IEEE/RSJ Int. Conf. Intell. Robot. Syst., Pittsburgh, 1995.

[8] J. Kim, B.J. Bettencourt, S.S. Krishnan, D.A. Paley, Control of autonomous underwater vehicles: A survey, IEEE J. Ocean. Eng. 38 (2013).

[9] B. Masoud, A. Meghdari, M.R. Firoozabadi, Dynamics Modeling and Control of an Autonomous Underwater Vehicle, Ocean Eng. 32 (2005).

[10] H. Goldstein, C. Poole, J. Safko, Classical Mechanics, Addison Wesley, 2002.